

Assessment of 3-D Printing Technologies for Millimeter-Wave Reflectors

Jordi Romeu , *Fellow, IEEE*, Sebastián Blanch , Neus Vidal ,
Josep Maria Lopez-Villegas, *Senior Member, IEEE*, and Albert Aguasca, *Member, IEEE*

Abstract—Three different 3-D printing technologies—stereolithography, fused deposition modeling, and HP Multi Jet Fusion technology—are compared to build a parabolic reflector operating at 100 GHz. Fabrication tolerance and surface roughness before and after metallization are accurately measured. The performance of the reflectors is measured in the near field, and it is compared against an optical grade reflector. In this way, the performance of the final product is thoroughly assessed.

Index Terms—Millimeter-wave devices, reflector antennas, three-dimensional printing.

I. INTRODUCTION

ADDITIONAL manufacturing technologies have become an effective alternative for the manufacturing of antennas. The major challenge in producing antennas in millimeter- and submillimeter-wave regions is to ensure the accuracy in the manufacturing [1], [2]. In addition, in the particular case of reflector manufacturing, the metallization process has to be also taken into account. Surface reflector roughness is a major source of gain reduction in a reflector. The well-known Ruze's formula [3] expresses the gain loss or reflector surface efficiency as

$$\Delta G = -685.81 \left(\frac{\epsilon}{\lambda} \right)^2 \text{ (dB)} \quad (1)$$

where ϵ is the root mean square (rms) surface error and λ is the wavelength. It means that at a frequency of 100 GHz, the rms error has to be smaller than $36 \mu\text{m}$ to have a gain loss smaller than 0.1 dB. Three-dimensional (3-D) printers have resolutions of the order of $10\text{--}100 \mu\text{m}$; therefore, it is interesting to measure the accuracy of different printing technologies to determine the upper frequency limit in which they can be used to print reflectors. To this end, three different printing technologies—stereolithography (SLA), fused deposition modeling (FDM), and HP Multi Jet Fusion (MJF) technology—are compared.

Manuscript received April 12, 2018; revised May 22, 2018 and June 29, 2018; accepted July 17, 2018. Date of publication; date of current version. This work was supported in part by the Spanish Inter-Ministerial Commission on Science and Technology (CICYT) under Grant TEC201678028-C3-1-P, Grant TIN2014-55413-C2-1-P, Grant TEC2017-85244-C2-2-P, and Grant TEC2017-83524-R, and in part by FEDER and the Unidat de Excelencia Maria de Maeztu under Grant MDM-2016-0600, which is financed by the Agencia Estatal de Investigación, Spain. (*Corresponding author: Jordi Romeu.*)

J. Romeu, S. Blanch, and A. Aguasca are with the Department of Signal Theory and Communications, CommSensLab, Universitat Politècnica de Catalunya (UPC), Barcelona 08034, Spain (e-mail: romeu@tsc.upc.edu; blanch@tsc.upc.edu; agasca@tsc.upc.edu).

N. Vidal and J. M. Lopez-Villegas are with the Department of Electronic and Biomedical Engineering, University of Barcelona, Barcelona 08007, Spain (e-mail: nvidal@ub.edu; j.m.lopez-villegas@ub.edu).

Digital Object Identifier 10.1109/LAWP.2018.2857856

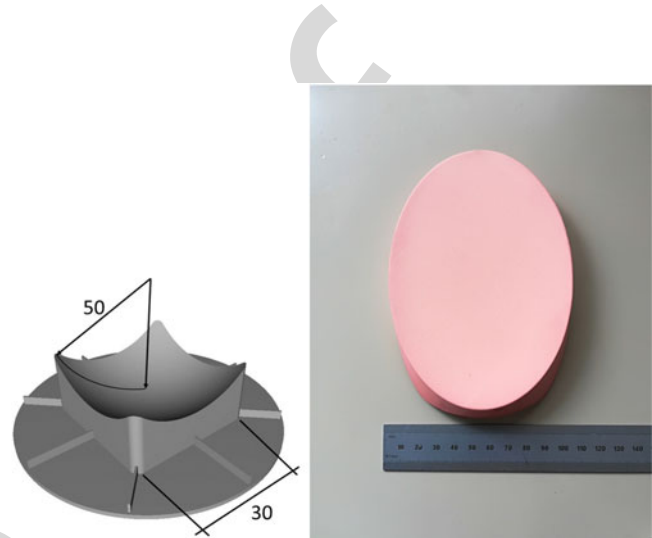


Fig. 1. Test object (left) and the metallized reflector (right).

A 90° offset parabolic reflector has been printed and metallized. The geometry of the reflector has been chosen to be the same as a commercial optical grade reflector, so their performance can be benchmarked against it. The mechanical accuracy of the printed and metallized surfaces has been measured by a confocal optical profiler that is able to provide accurate contactless surface profiles. Finally, a planar near-field scan of the reflectors has been done to assess their electromagnetic performance. The paper is organized as follows. In Section II, the 3-D printing, metallization, and mechanical verification of the printed reflectors are described. In Section III, the electromagnetic behavior of the reflectors is presented, and finally, the conclusions are presented in Section IV.

II. MANUFACTURING PROCESS

A. 3-D Printing and Metallization

Two sets of objects have been printed and metallized. The first is the test object shown in Fig. 1 (left). It is a sphere of radius 50 mm intersected with a cube of 30 mm side. This test object has the advantage that its measured profile can be easily compared with the theoretical one.

The second object shown in Fig. 1 (right) is a 90° offset reflector of 101.6 mm diameter with a parent focal length of 76.2 mm. This geometry has been chosen to be the same as commercial optical grade reflector made by Edmund Optics that will be used as a benchmark for the 3-D-printed reflectors. The reference parabolic reflector has nominal rms roughness smaller than $0.01 \mu\text{m}$ and has an Aluminum 6061-T6 coating with a

TABLE I
SURFACE ERROR FOR THE TEST OBJECT

Name	Printing Technology	Material	Finishing	Surface error rms (μm)
FDM	FDM	PLA	None	27.6
FDM+Cu	FDM	PLA	Sanding, Metallization	13.8
SLA+Cu	SLA	Therma 294	Metallization	8.8
MJF1	MJF	PA 12	Sand Blasting	24.5
MJF2	MJF	PA 12	Tumbling	12.2
MJF3	MJF	PA 12 GB	Sand Blasting	36
MJF4	MJF	PA 12 GB	Tumbling	25.6

62 conductivity of $2.5 \cdot 10^7$ S/m. The SLA objects have been printed
 63 using a XFAB Stereolithographic 3-D printer from DWS. The
 64 base material is a nanoceramic-filled photopolymer Therma
 65 294 that allows high resolution modeling (10–100 μm layer
 66 thickness). For the FDM, a SIGMA 3-D printer manufactured
 67 by BCN3D with a step resolution of 100 μm has been used and
 68 the objects have been printed on polylactide (PLA). Finally, an
 69 HP 3-D MJF 4200 has been used to print the objects on two
 70 different materials PA 12 and PA 12 GB. These are thermoplastics
 71 the second one with a loading of glass beads to increase the
 72 mechanical stability. The MJF printed objects have been given
 73 two different finishing processes, sandblasting and tumbling, to
 74 reduce the surface roughness. The metallization process is by
 75 copper electrodeposition by electrolysis. A 17 μm thick layer
 76 of copper is deposited following the process described in [4].
 77 Further testing has shown that this method provides surface
 78 resistances close to the ones obtained from copper, in particular
 79 accurate cavity measurements at 9 GHz have shown a surface
 80 resistance of 35.93 $\text{m}\Omega$ for electrodeposited copper on PLA
 81 compared to 25.68 $\text{m}\Omega$ for pure copper [5].

82 B. Mechanical Verification

83 The accuracy of the printed objects has been verified by a
 84 Plu Neox Optical Profiler manufactured by Sensofar Metrology
 85 [6]. The measurement principle is described in [7] and it
 86 allows contactless high accuracy profile measurements that include
 87 submicron surface roughness measurements. The goal of the
 88 mechanical verification is to have a measurement of the surface
 89 roughness as well as deviations from the specified nominal shape.
 90 To this end, accurate profiles of the test object of Fig. 1 (left)
 91 have been measured before and after metallization. The description
 92 of each object is shown in Table I and the measured results are
 93 shown in Fig. 2. For each one of the test objects, the measured
 94 profile compared to the theoretical one is shown on the left of the
 95 figure. On the right, the surface error is shown. From this error
 96 curve, the rms surface error is found and it is shown in Table I.
 97 The results show that the best roughness is obtained by the SLA
 98 printed object that has a roughness of 8 μm after metallization.
 99 The profile measurements of Fig. 2 also show the effects on the
 100 surface of the applied surface treatment. In the case of the MJF
 101 samples, sandblasting or tumbling has been applied. It is observed
 102 that these surface treatments smoothen the surface, but they can
 103 leave residual surface errors. In the

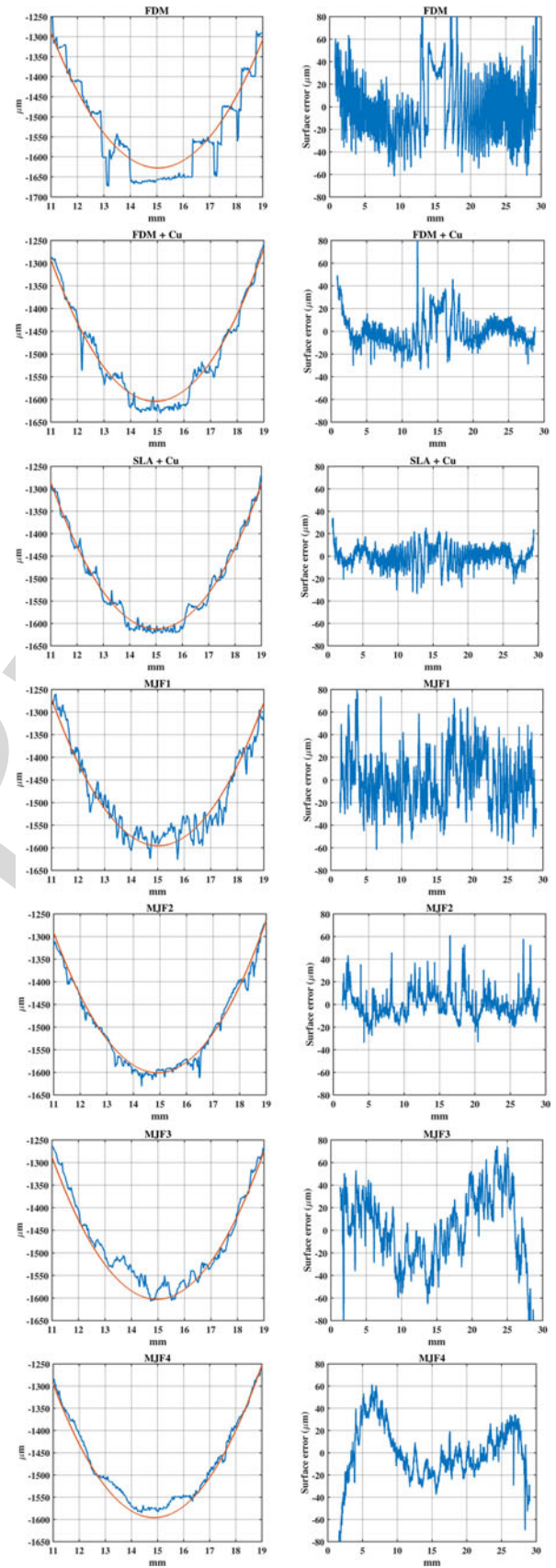


Fig. 2. Profile measurement results for the test object (left) and surface error (right).

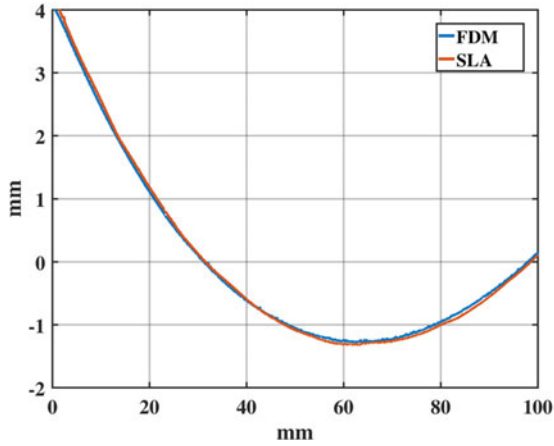


Fig. 3. Profile measurement of the metallized FDM and SLA printed reflectors.

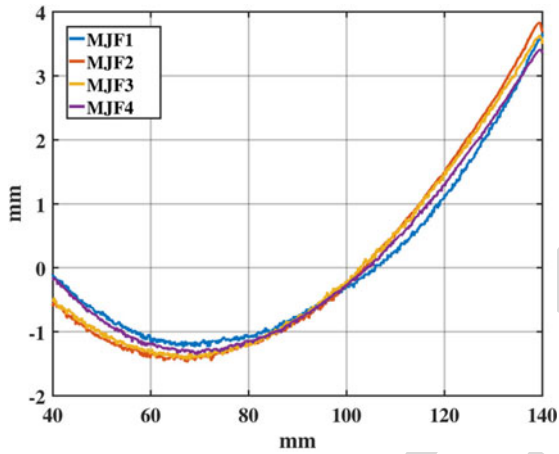


Fig. 4. Profile measurement of the metallized MJF printed reflectors.

104 case of the FDM object, the $100\ \mu\text{m}$ vertical steps of the printer
 105 are clearly observable. For this object, prior to the metallization,
 106 it has been smoothed with a fine grain sandpaper. Therefore,
 107 the resulting metallized object has a smoother texture. In all
 108 cases, the surface roughness is below the $36\ \mu\text{m}$ design goal for
 109 a 100 GHz reflector.

110 Once the reflectors have been printed and metallized, and be-
 111 fore proceeding to the EM testing, their profile has also been
 112 measured with the optical profiler. Due to the large dimension
 113 of the reflector, a partial profile along the vertical dimension
 114 has been measured. In Fig. 3, the profiles for the FDM and
 115 SLA printed and metallized reflectors are compared. In Fig. 4,
 116 the profiles for the four MJF reflectors are compared. The first
 117 evident conclusion is that the four MJF reflectors present clear
 118 differences in their profiles. It is also evident that their rough-
 119 ness is higher than in the FDM and SLA printed reflectors. For
 120 unknown reasons, that has to be further investigated as some of
 121 the MJF reflectors have suffered some deformation during the
 122 printing process.

123 III. EM TESTING

124 In order to assess the performance of the reflectors, their radia-
 125 tion pattern has been measured using a planar near field scanning
 126 technique at a frequency of 100 GHz. The measurement setup

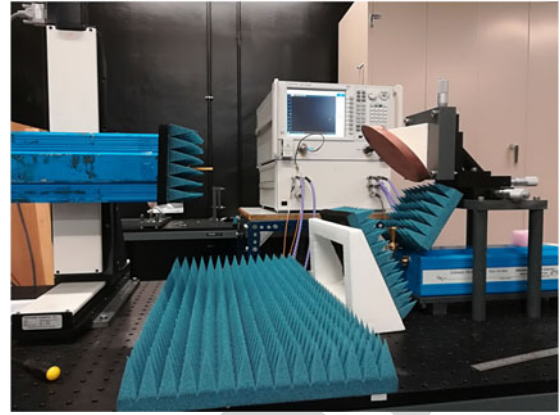


Fig. 5. Near-field scanning of a printed reflector.

is shown in Fig. 5 where one of the 3-D printed reflectors is tested.

The H plane pattern (horizontal cut according to the measure-
 ment setup of Fig. 5) for all the reflectors is shown in Fig. 6. In
 Table II, the directivity and the normalized radiated power for
 each reflector compared to the reference optical grade reflector
 is shown. Notice that, in this case, all the printed reflectors have
 been metallized. The observation of the radiation patterns shows
 similar cross-polar level in all cases. The changes in directivity
 can be as high as $-0.80\ \text{dB}$ compared to the optical grade
 reflector and the reflector that better matches the performance
 of the optical grade reflector is the FDM. The total radiated
 power has been compared from the integration of the field compo-
 nents in the near-field measurements. It is interesting to note
 that the radiated power for the 3-D printed reflectors is higher
 than the power radiated by the optical grade reflector in all cases.

This fact can be explained due to the lower surface resistance
 of the copper metallization compared to the aluminum coating
 of the optical reflector. In addition, the thickness of the alu-
 minum coating of the optical grade reflector is not known, but it
 is also possible that the coating thickness is smaller than $30\ \mu\text{m}$,
 which is the penetration depth at 100 GHz, finally the fact
 that the optical grade reflector has sharper edges that probably
 contribute to higher edge diffraction. The radiated power is
 obtained from the planar near-field measurement; therefore, the
 scattered power is not properly taken into account. In Table II,
 the measured roughness for each reflector is also shown. This
 roughness has been measured following the procedure of [8].
 The roughness is the rms height after removing the primary sur-
 face. The specific way in which it has been computed involves
 two steps. First an error function is obtained by subtracting the
 desired parabolic curve from the measured profile. Then the rms
 value of the error function is obtained after applying a spatial
 low pass filter of 2 mm cutoff length. It is observed that after
 metallization, the surface roughness is below $21\ \mu\text{m}$ in all cases.
 As expected from the results of Figs. 3 and 4, the roughness for
 the SLA and FDM reflectors is smaller. It is also observed that
 the H plane 3 dB beam width (horizontal plane) is practically
 the same in all cases, and differences of the order of 0.1° can
 be observed in the E plane. Of course the larger beam width in-
 crements correspond to the largest decrements in directivity. Due
 to the similar surface roughness, we think that the directivity
 reduction is produced by larger scale surface errors. As shown

127
 128
 129
 130
 131
 132
 133
 134
 135
 136
 137
 138
 139
 140
 141
 142
 143
 144
 145
 146
 147
 148
 149
 150
 151
 152
 153
 154
 155
 156
 157
 158
 159
 160
 161
 162
 163
 164
 165
 166
 167
 168
 169
 170



Q3

Q4

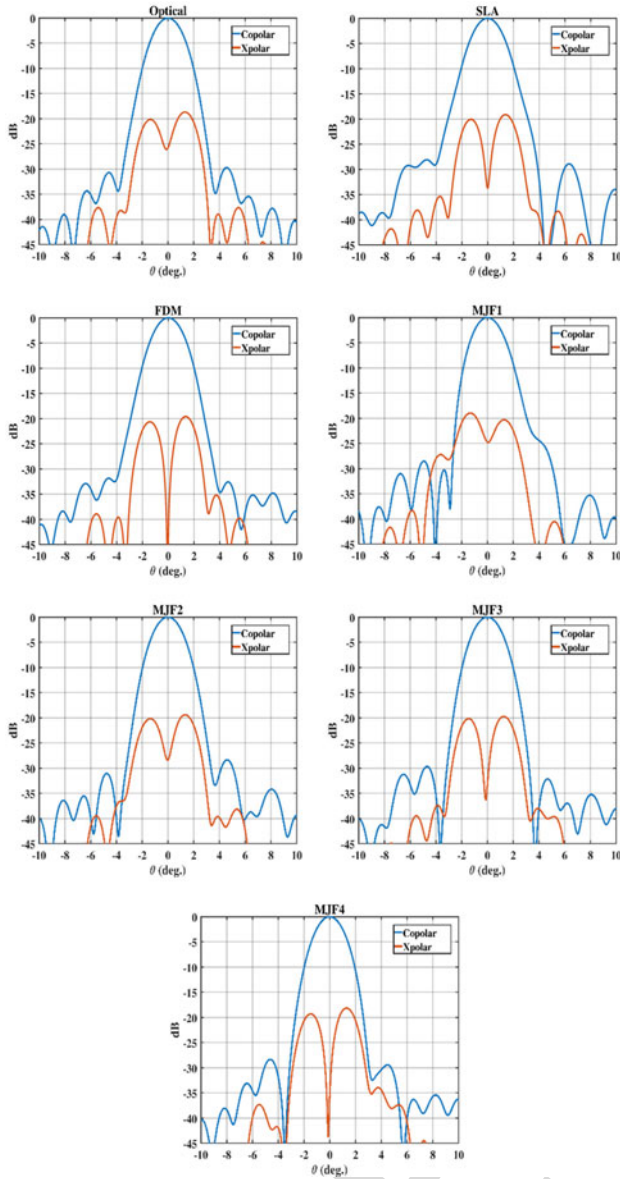


Fig. 6. H plane radiation pattern for each reflector.

in Fig. 4, the profiles of the MJM-printed reflectors exhibit large differences. As a matter of fact, MJM2 and MJM3 have similar profiles and their directivity loss compared to the optical reflector is similar. On the other hand, MJM1 and MJM4 have more different profiles that we must infer that have higher deviation from the nominal surface that result in higher directivity losses.

Assuming that the FDM reflector is the one that better reproduces the nominal reflector shape, the comparison of Fig. 3 shows that the SLA profile has a ripple around the nominal shape. For practical reason, the SLA reflector was printed vertically and that resulted in this ripple that can be the cause of the directivity reduction.

TABLE II
MEASURED RADIATION PARAMETERS

Name	D (dB)	$\Delta\theta_{3dB}$ E-plane (°)	$\Delta\theta_{3dB}$ H-plane (°)	Relative Directivity (dB)	Relative Radiated Power (dB)	Roughness (μm)
Optical	38.84	2.02	2.22	0	0	0.01 ¹
FDM	38.83	2.03	2.26	-0.01	0.21	9.6
SLA	38.33	2.13	2.27	-0.51	0.56	8
MJF1	38.39	2.13	2.23	-0.45	0.34	17
MJF2	38.61	2.07	2.23	-0.23	0.2	14
MJF3	38.69	2.05	2.23	-0.15	0.4	21
MJF4	38.04	2.18	2.22	-0.80	0.36	14

¹ Nominal value

IV. CONCLUSION

The potentiality of 3-D printing of parabolic reflectors for being used in frequencies in the 100 GHz band has been shown. Accurate surface measurements have shown that the metallized reflectors can achieve surface roughness of the order of 10 μm . According to Ruze's equation, a reflector with such roughness could be used for frequencies up to 300 GHz with gain losses of 0.1 dB. Nevertheless, the measurements have shown that although the local roughness can achieve these low values, there may be other larger scale surface errors that can degrade the performance of the reflector. In particular, the best results have been obtained with the FDM reflector that has almost the same performance as the optical grade reflector. In this case, although the printing resolution is not the best, the fact that the printing material is relatively soft leads to easy smoothing by hand sanding. Also the printing material PLA does not need high temperatures and that may explain the smaller deformation of the printed reflector as compared to the HP MJF reflectors.

REFERENCES

- [1] E. A. Rojas-Nastrucci, J. T. Nussbaum, N. B. Crane, and T. M. Weller, "Ka-Band characterization of binder jetting for 3-D printing of metallic rectangular waveguide circuits and antennas," *IEEE Trans. Microw. Theory Techn.*, vol. 65, no. 9, pp. 3099–3108, Sep. 2017, doi: 10.1109/TMTT.2017.2730839.
- [2] B. Zhang, Y. X. Guo, H. Zirath, and Y. P. Zhang, "Investigation on 3-D-printing technologies for millimeter-wave and terahertz applications," in *Proc. IEEE*, 2017, vol. 105, no. 4, pp. 723–736, doi: 10.1109/JPROC.2016.2639520.
- [3] J. Ruze, "Antenna tolerance theory—A review," in *Proc. IEEE*, 1966, vol. 54, no. 4, pp. 633–640, doi: 10.1109/PROC.1966.4784.
- [4] J. Romeu, A. Aguasca, S. Blanch, J. O'Callaghan, L. Jofre, and S. Buitrago, "A submillimeter wave parabolic reflector by additive manufacturing," in *Proc. Accepted IEEE Antennas Propag. Soc. Symp.*, Boston, 2018.
- [5] P. Krkotic, A. Aguasca, and J. M. O'Callaghan, "Small footprint evaluation of metal coatings for additive manufacturing," in *Proc. Submitted Eur. Microw. Conf.*, Madrid, 2018.
- [6] Sensofar Group. [Online]. Available: www.sensofar.com
- [7] R. Artigas, A. Pintó, and F. Laguarda, "Three-dimensional micromerements on smooth and rough surfaces with a new confocal optical profiler SPIE," in *Proc. Int. Soc. Opt. Eng.*, 1999, vol. 3824, pp. 93–104.
- [8] *Geometrical Product Specifications (GPS)—Surface Texture: Areal—Part 2: Terms, Definitions and Surface Texture Parameters*, ISO 25178-2:2012(en).

- **Authors: We cannot accept new source files as corrections for your paper. If possible, please annotate the PDF proof we have sent you with your corrections and upload it via the Author Gateway. Alternatively, you may send us your corrections in list format. You may also upload revised graphics via the Author Gateway.**

QUERIES

- Q1. Author: Please confirm or add details for any funding or financial support for the research of this article. 233
- Q2. Author: The sense of the sentence “these are thermoplastics” is not clear. Please check that it reads correctly and supply a revised version if necessary. 234
235
- Q3. Author: Please provide the expansion of EM at first mention. 236
- Q4. Author: The sense of the sentence “In addition, the thickness” is not clear. Please check that it reads correctly and supply a revised version if necessary. 237
238
- Q5. Author: Please provide page range for Refs. [4] and [5]. 239
- Q6. Author: Please check whether Ref. [6] is okay as set. 240

Response to the Queries

Q1. We confirm the funding support information is correct.

Q2. Please replace "These are thermoplastics" by "These two materials are thermoplastics".

Q3. Electro Magnetic (EM)

Q4. Delete "In addition," Start the sentence by " The thickness of ...

Q5. For ref [4] 2018 IEEE International Symposium on Antennas and Propagation & USNC/URSI National Radio Science Meeting, Boston, MA, 2018, pp. 937.

for ref [5] it has been accepted but not published yet (the conference is in September '18) so we do not have the page number yet. Please cite it as "accepted to the 2018 48th European Microwave Conference (EuMC), Madrid, 2018"

Q6. Yes ref [6] is correct.